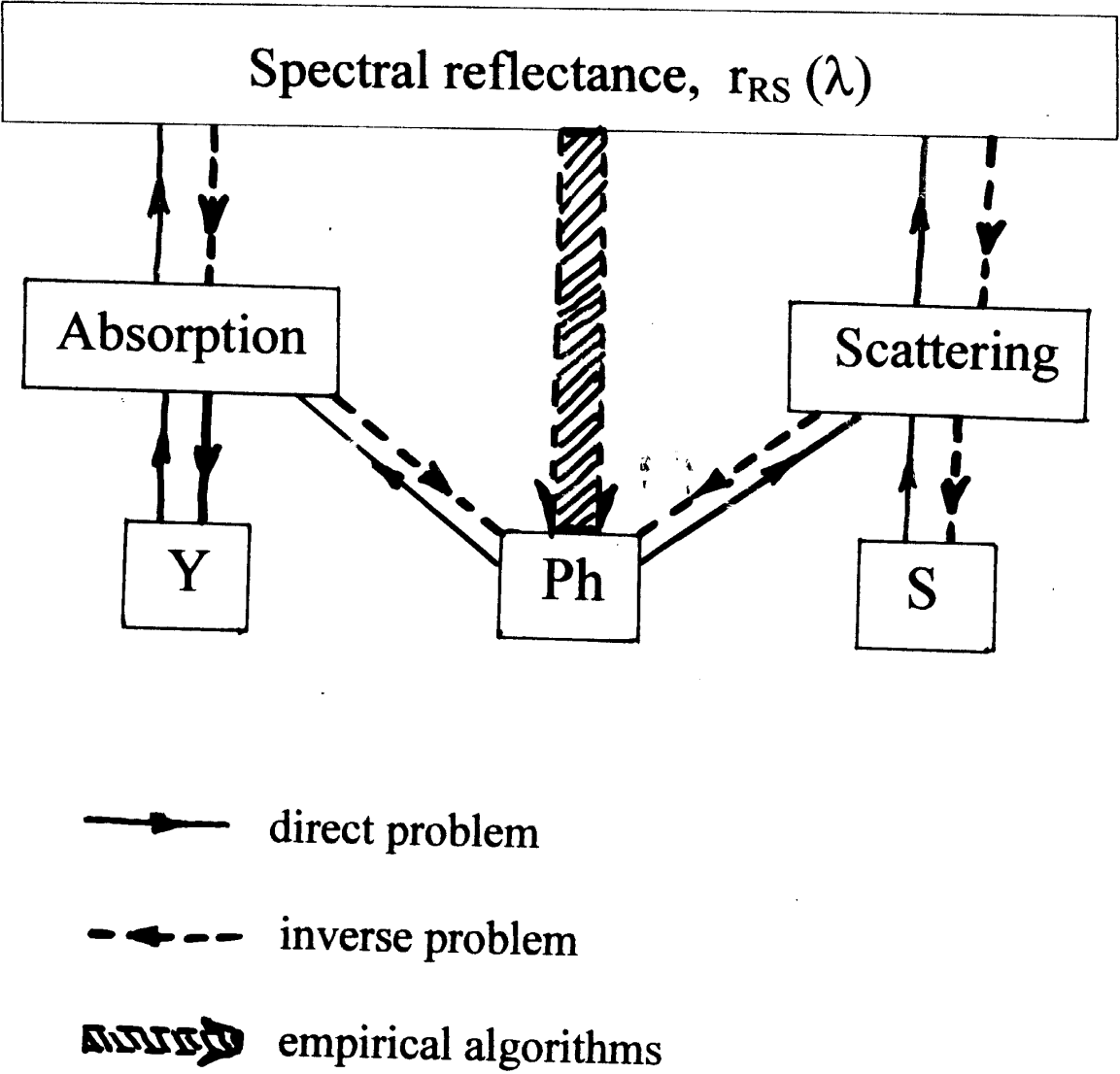O. Kopelevich

Topic 8:   Bio-optical algorithms

Empirical models

Semianalytic algorithms

Results of algorithm validation

Relationships between spectral reflectance, seawater optical properties, and in-water constituents

Spectral reflectance, $r_{RS}(\lambda)$

Absorption

Scattering

Y

Ph

S

⟶ direct problem

⟵ inverse problem

empirical algorithms

The empirical algorithms are based on direct regression of the ratio of reflectances at two wavelengths λ_1 and λ_2 to chlorophyll concentration Chl:

Regression equations:

$$\text{Chl} = f\ \{a_0;\ a_1;\ldots;\ a_5;\ [r_{RS}(\lambda_1)/r_{RS}(\lambda_2)]\}\ ;$$

$a_0, a_1, \ldots, a_5$ are the regression coefficients;

λ_1 is usually 443 or 490 nm;

λ_2 is 550 or 555 nm.

The log-transformed data are commonly used and different forms of the regression equation have been employed: power, hyperbolic, cubic, multiple regression.

Table 2. Empirical Algorithms (O'Reilly et al. 1998)

	Algorithm	Type	Result Equation(s)	Band Ratio (R), Coefficients (a)	Reference
1.	Global processing (GPs)	power	$C_{13} = 10^{(a0 + a1*R1)}$ $C_{23} = 10^{(a2 + a3*R2)}$ $[C + P] = C_{13}$; if C_{13} and $C_{23} > 1.5$ μg L^{-1} then $[C + P] = C_{23}$	$R1 = \log(Lwn443/Lwn550)$ $R2 = \log(Lwn520/Lwn550)$ $a = [0.053, -1.705, 0.522, -2.440]$	1
2.	Clark three-band (C3b)	power	$[C + P] = 10^{(a0 + a1*R)}$	$R = \log((Lwn443 + Lwn520)/Lwn550)$ $a = [0.745, -2.252]$	2
3.	Aiken-C	hyperbolic + power	$C_{21} = \exp(a0 + a1*\ln(R))$ $C_{23} = (R + a2)/(a3 + a4*R)$ $C = C_{21}$; if $C < 2.0$ μg L^{-1} then $C = C_{23}$	$R = Lwn490/Lwn555$ $a = [0.464, -1.989, -5.29, 0.719, -4.23]$	3
4.	Aiken-P	hyperbolic + power	$C_{22} = \exp(a0 + a1*\ln(R))$ $C_{24} = (R + a2)/(a3 + a4*R)$ $[C + P] = C_{22}$; if $[C + P] < 2.0$ μg L^{-1} then $[C + P] = C_{24}$	$R = Lwn490/Lwn555$ $a = [0.696, -2.085, -5.29, 0.592, -3.48]$	3
5.	OCTS-C	power	$C = 10^{(a0 + a1*R)}$	$R = \log((Lwn520 + Lwn565)/Lwn490)$ $a = [-0.55006, 3.497]$	4
6.	OCTS-P	multiple regression	$[C + P] = 10^{(a0 + a1*R1 + a2*R2)}$	$R1 = \log(Lwn443/Lwn520)$ $R2 = \log(Lwn490/Lwn520)$ $a = [0.19535, -2.079, -3.497]$	5
7.	POLDER	cubic	$C = 10^{(a0 + a1*R + a2*R^2 + a3*R^3)}$	$R = \log(Rrs443/Rrs565)$ $a = [0.438, -2.114, 0.916, -0.851]$	6
8.	CalCOFI two-band linear	power	$C = 10^{(a0 + a1*R)}$	$R = \log(Rrs490/Rrs555)$ $a = [0.444, -2.431]$	7
9.	CalCOFI two-band cubic	cubic	$C = 10^{(a0 + a1*R + a2*R^2 + a3*R^3)}$	$R = \log(Rrs490/Rrs555)$ $a = [0.450, -2.860, 0.996, -0.3674]$	7
10.	CalCOFI three-band	multiple regression	$C = \exp(a0 + a1*R1 + a2*R2)$	$R1 = \ln(Rrs490/Rrs555)$ $R2 = \ln(Rrs510/Rrs555)$ $a = [1.025, -1.622, -1.238]$	7
11.	CalCOFI four-band	multiple regression	$C = \exp(a0 + a1*R1 + a2*R2)$	$R1 = \ln(Rrs443/Rrs555)$ $R2 = \ln(Rrs412/Rrs510)$ $a = [0.753, -2.583, 1.389]$	7
12.	Morel-1	power	$C = 10^{(a0 + a1*R)}$	$R = \log(Rrs443/Rrs555)$ $a = [0.2492, -1.768]$	8
13.	Morel-2	power	$C = \exp(a0 + a1*R)$	$R = \ln(Rrs490/Rrs555)$ $a = [1.077835, -2.542605]$	9
14.	Morel-3	cubic	$C = 10^{(a0 + a1*R + a2*R^2 + a3*R^3)}$	$R = \log(Rrs443/Rrs555)$ $a = [0.20766, -1.82878, 0.75885, -0.73979]$	9
15.	Morel-4	cubic	$C = 10^{(a0 + a1*R + a2*R^2 + a3*R^3)}$	$R = \log(Rrs490/Rrs555)$ $a = [1.03117, -2.40134, 0.3219897, -0.291066]$	9

References: 1, *Evans and Gordon* [1994]; 2, *Muller-Karger et al.* [1990]; D. Clark; *McClain and Yeh* [1994]; 3, *Aiken et al.* [1995]; 4, Science on the GLI Mission, p. 16; Ocean Optics XIII, Halifax, October 1996; 5, Ocean Optics XIII, Halifax, October 1996; personal communication to C.
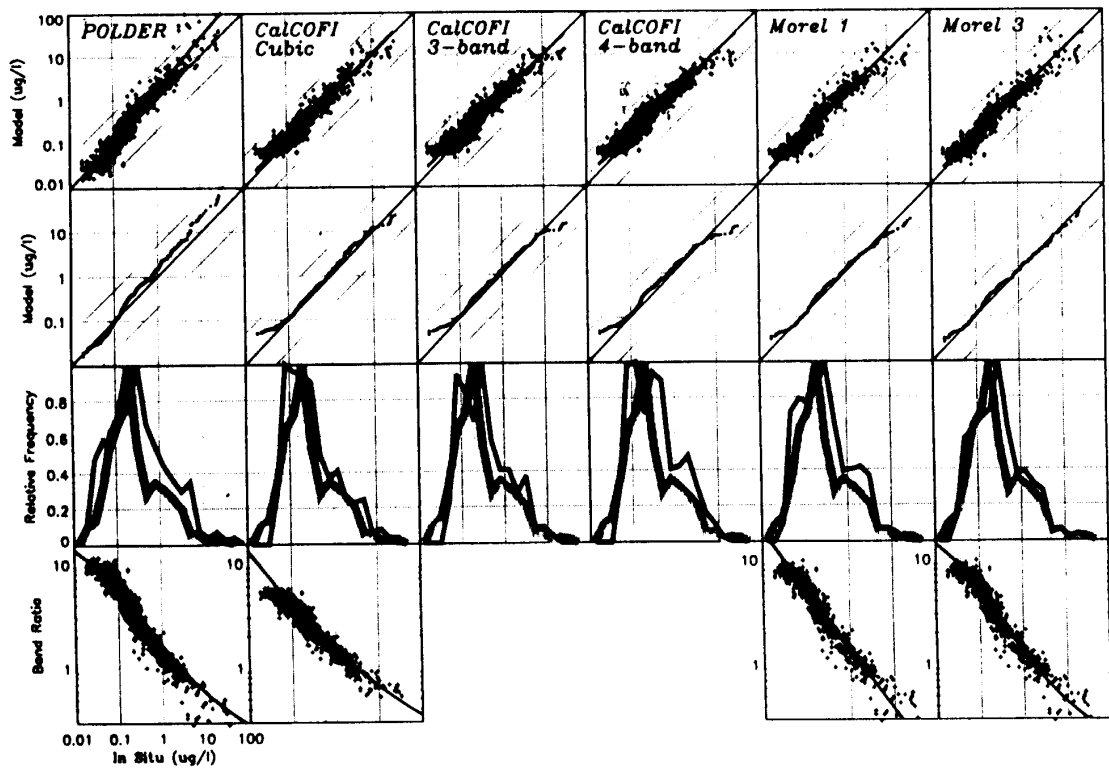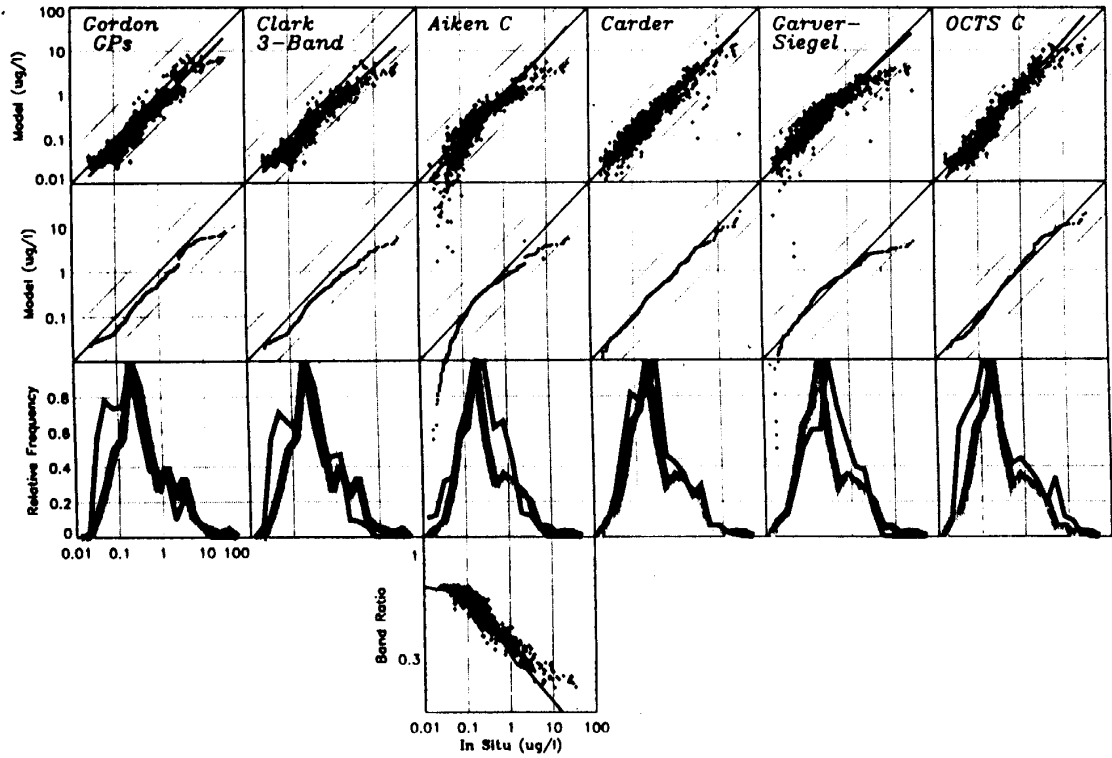
Figure 4. Comparisons between model and in situ data: (top) Gordon GPS, Clark three-band, Aiken-C, Carder (global), Garver/Siegel (global), and OCTS-C models; (bottom) POLDER, CalCOFI cubic, CalCOFI three-band, CalCOFI four-band, Morel-1, and Morel-3 models. From top to bottom: Scatterplots; quantile-quantile plots; relative frequency of model (thin black line) and in situ (thick faint line); band ratio versus in situ C for two-band ratio algorithms (pluses) and band ratio versus model (curve). Note that the axes for each row of figures are shown in column 1. Also shown are lines indicating model:in situ ratios of 1:5 and 5:1.

(O'Reilly et al. 1998)

SeaBAM Data Set

Table 3. Data Sources and Characteristics of SeaBAM Data Set

Data Set	Provider/PI	Location	Date	n	f_{chla}	f_{phaeo}	h_{chla}	h_{phaeo}	Wavelength
BBOP92-93	D. Siegel	Sargasso Sea	monthly, 1992–1993	72	72	72	72		410, 441, 488, 520, 565, 665
BBOP94-95	D. Siegel	Sargasso Sea	monthly, 1994–1995	67	61	61	67		410, 441, 488, 510, 555, 665
WOCE	J. Marra	50°S–13°N, 88°–91°W 10°S–30°N, 18°–37°W	March 1993 April 1994	70	70				410, 441, 488, 520, 565, 665
EQPAC	C. Davis	0, 140°W	March and Sept. 1992	126			126		410, 441, 488, 520, 550, 683
NABE	C. Trees	46°–59°N, 17°–20°W	May 1989	72			72		412, 441, 488, 521, 550 ···
NABE	C. Davis	46°N, 19°W	April 1989	40			40		410, 441, 488, 520, 550, 683
CARDER	K. Carder	North Atlantic Pacific Gulf Mexico Arabian Sea	Aug. 1991 July 1992 April 1993 Nov. 1994 and June 1995	87	87				412, 443, 490, 510, 555, 670
CALCOFI	G. Mitchell	California Current	quarterly, Aug. 1993 to July 1996	303	303	303			412, 443, 490, 510, 555, 665
MOCE1	D. Clark	Monterey Bay	Sept. 1992	8	8	0	8		412, 443, 490, 510, 555 ···
MOCE2	D. Clark	Gulf California	April 1993	5	5	5	5		412, 443, 490, 510, 555 ···
North Sea	R. Doerffer	55°–52°N, 0°–8°E	July 1994	10			10		412, 443, 490, 510, 555, 670
Chesapeake Bay	L. Harding	~37°N, 75°W	April and July 1995	9			9	9	412, 443, 490, 510, 555, 671
Canadian Arctic	G. Cota	~74.38°N, 95°W	August 1996	8	8	7			412, 443, 490, 509, 555, 665
AMT	G. Moore	50°N–50°S	Sept. 1995 and April 1996	42	42		33		412, 443, 490, 510, 555 ···
Total				919	656	448	442	9	

f_{chla}: fluorometric chlorophyll a; f_{phaeo}: fluorometric phaeophytin a; h_{chla}: HPLC chlorophyll a; h_{phaeo}: HPLC phaeophytin a.
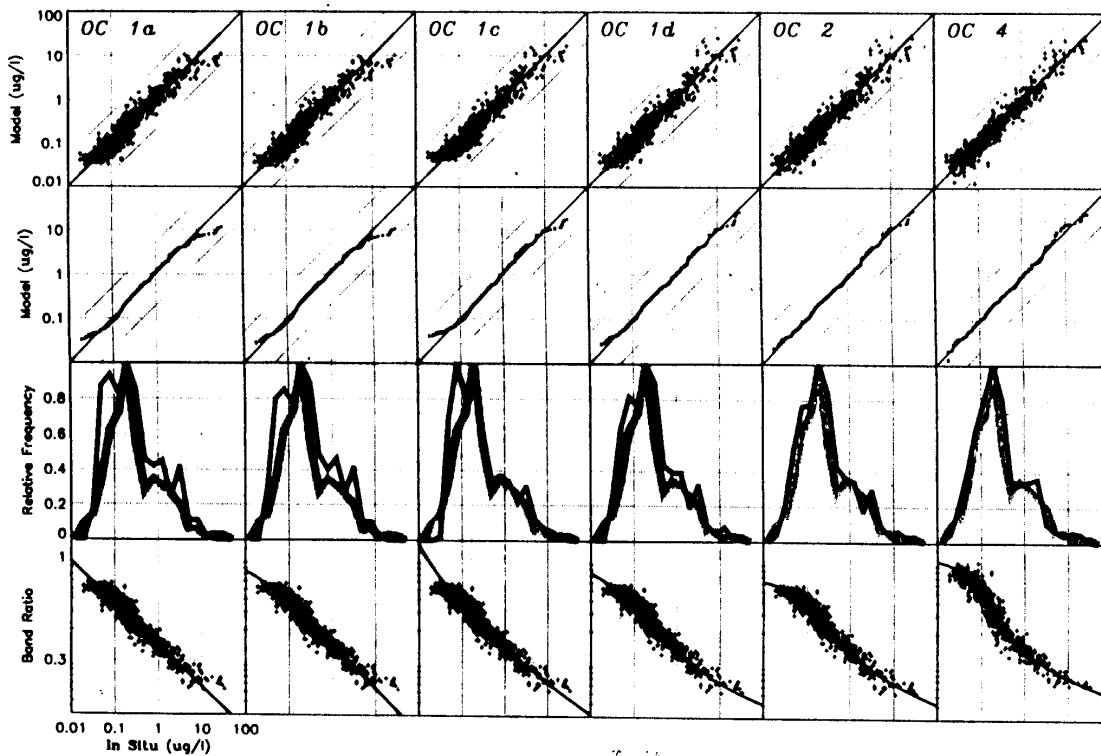
Figure 5. Comparisons between models tuned to the SeaBAM data set and in situ data: OC1a (power), OC1b (geometric), OC1c (quadratic polynomial), OC1d (cubic polynomial), OC2 (modified cubic polynomial), and OC4 (maximum band ratio) algorithms. See Figure 4 caption for additional details.

The updated OC2 algorithm is as follows :

$$[chl-a] = 10^{\left(0.2974 -2.2429*R + 0.8358*R^2 -0.0077*R^3\right)} - 0.0929$$

with $R = \log_{10}(R_n(490)/R_n(555))$.

(the coefficients were derived by fitting to an extended version of the SeaBAM data set).

Why is band ratio?   What bands are taken?

1. The remote-sensing reflectance can be assumed as proportional to b_b/a; so if the band ratio is taken, the influence of scattering is weakened:

$$r_{RS}(\lambda_1)/r_{RS}(\lambda_2) \sim [b_b(\lambda_1)/b_b(\lambda_2)] \cdot [a(\lambda_2)/a(\lambda_1)] \sim [a(\lambda_2)/a(\lambda_1)].$$

2. λ_1 is taken from the interval of 400-500 nm, which is a broad absorption band of phytoplankton pigment, λ_2 is from 500-600 nm which is an interval with low pigment absorption. Because the yellow substance absorption is also low in the interval of 500-600 nm in open ocean, absorption at λ_2 can be taken as constant (equal to absorption by pure water):

$$r_{RS}(\lambda_1)/r_{RS}(\lambda_2) \sim 1/a(\lambda_1).$$

3. The absorption at λ_1 is caused not only by phytoplankton but also by yellow substance. It is assumed that the definite relationship exists between the chlorophyll absorption and the yellow substance absorption, so the total absorption (ignoring absorption by pure water) can be taken as proportional to chlorophyll concentration:

$$a(\lambda_1) \sim Chl, \qquad\qquad r_{RS}(\lambda_1)/r_{RS}(\lambda_2) \sim 1/a(\lambda_1) \sim 1/Chl.$$

$$\mathcal{r}_{RS}(\lambda_1)/\mathcal{r}_{RS}(\lambda_2)$$
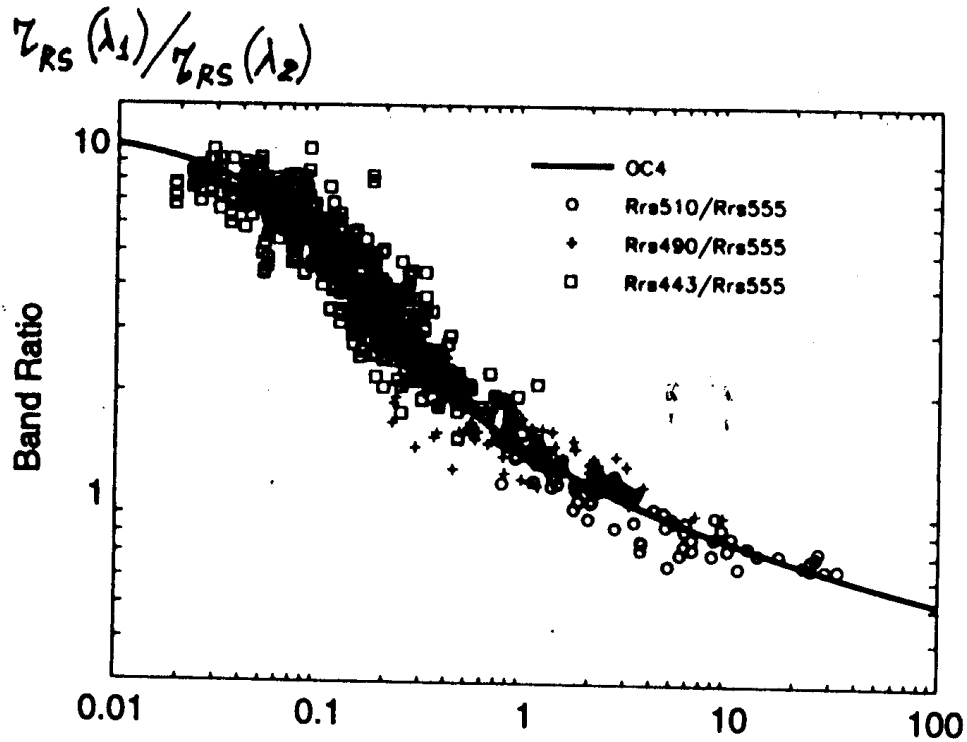
Chl, mg·m^{-3}

(O'Reilly et al. 1998).

The regressional algorithms are only applicable to Case 1 waters with a definite relationship between the absorption by phytoplankton pigments and by yellow substance. If some additional amount of yellow substance appears in water with no increasing chlorophyll concentration, it results in increasing $a(\lambda_1)$ and thus decreasing the band ratio. The empirical algorithm attributes such decreasing to increase of chlorophyll concentration and derives its overestimated value.

Comparison between chlorophyll a concentrations (mg m^{-3}) measured and retrieved by the semianalytic and the operational SeaWiFS algorithms at different stations in the Black Sea (St.1-3) and the Aegean Sea (St. 4, 5); β is the ratio between the absorption coefficients of gelbstoff and phytoplankton pigments at 440 nm.

St.	Coordinates	Chl in situ	Chl semianalytic	Chl SeaWiFS	β
1	42.51 N, 39.52 E	0.35	0.23	0.68	4.3
2	42.96 N, 35.60 E	0.57	0.56	1.20	3.4
3	42.90 N, 31.60 E	0.45	0.56	1.12	2.6
4	39.32 N, 25.12 E	0.089	0.086	0.21	5.9
5	39.61 N, 25.79 E	0.076	0.088	0.18	5.2

The ratio *b* can be used as an indicator of validity of the SeaWiFS bio-optical algorithm which assumes a definite relationship between the absorption by phytoplankton pigments and absorption by yellow sunstance. The SeaWiFS algorithm overestimates chlorophyll concentration if the ratio *b* exceeds the critical value which is about 2. In the Black and Aegean Seas where the *b* values are 2.6-5.9 the SeaWiFS algorithm overestimates the chlorophyll concentration about twice.
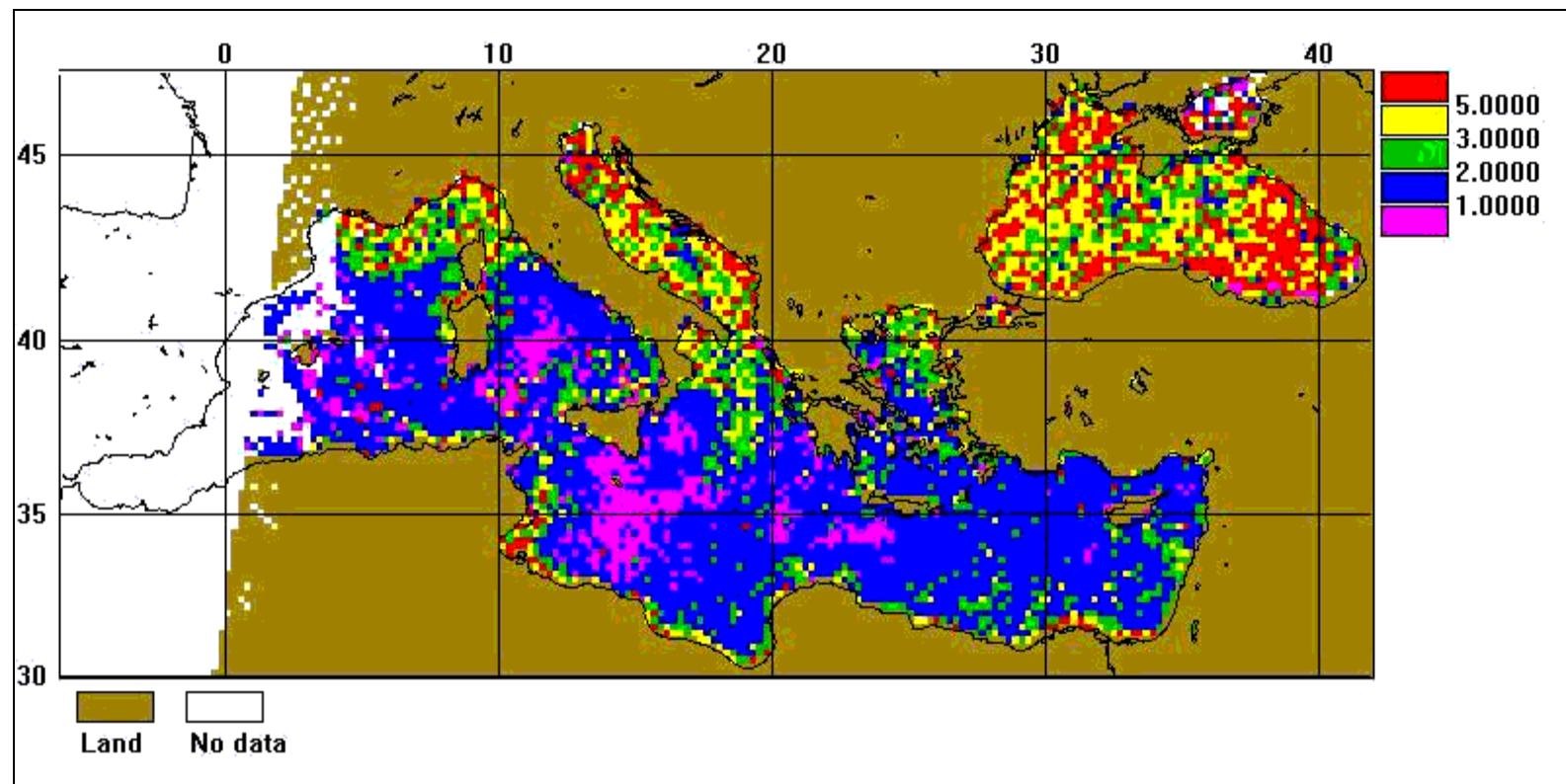
The mean distribution of *b*-values in the Mediterranean and Black Seas over September-October 1997 derived from SeaWiFS data (the measurements at St.1-5 were conducted in the beginning of October 1997).

Comparison between chlorophyll-a concentrations (mg·m^{-3}) measured and retrieved by the semianalytic and the operational SeaWiFS algorithms at different stations in the Barents Sea. β is the ratio between the absorption coefficients of yellow substance and phytoplankton pigments at 440 nm.

St.	Coordinates	Chl measured	Chl semianalytic	Chl SeaWiFS	β
1088	70.42 N, 47.58E	0.16	0.24	0.63	8.2
1090	70.18N, 52.42E	0.50	0.56	3.3	14.9
1095	68.97N, 58.47E	0.79	0.34	9.9	20.9
1112	69.09N, 58.29E	0.42	0.46	9.5	35.9
1123	69.50N, 57.25E	0.38	0.55	4.8	22.9
1126	69.67N, 57.24E	0.18	0.114	2.7	25.5
1131	69.77N, 56.28E	0.091	0.038	1.01	14.7
1157	70.54N, 52.79E	0.25	0.14	1.09	8.7
1174	69.25N, 41.00E	1.39	0.92	1.0	1.6
1183	71.50N, 41.00E	0.38	0.38	0.81	3.2
1196	74.75N, 41.00E	0.13	0.14	0.28	4.1
1209	78.00 N, 41.00E	0.16	0.17	0.25	3.0
1281	76.00N, 42.27E	0.27	0.38	0.44	3.2

Semianalytic algorithms

The top-of-the-atmosphere reflectance $R_t(\lambda_i)$

Atmospheric correction

Above-surface reflectance $R_{RS}(\lambda_i)$ or $L_{WN}(\lambda_i) = R_{RS}(\lambda_i) \cdot F_o(\lambda_i)$.

$$R_{RS} = (t_- \, t_+ / n^2) \cdot r_{RS} / (1 - \gamma R)$$

Subsurface reflectance $r_{RS}(\lambda_i)$

$$r_{RS} \approx (0.070 + 0.155 \, X^{0.752}) \, X$$

Parameter $X(\lambda_i)$

$$X(\lambda_i) = b_b(\lambda_i) / [a(\lambda_i) + b_b(\lambda_i)]$$

Seawater absorption and backscattering $a(\lambda_i)$ and $b_b(\lambda_i)]$

Low-parametric models

Seawater constituents Chl, Y, and S

SIORAS algorithm for SeaWiFS

$$\mathcal{L}_{WN}(\lambda_i) \rightarrow X(\lambda_i) = \frac{b_6(\lambda_i)}{a(\lambda_i) + b_6(\lambda_i)};$$

$$i = 1, 2, \ldots, 5$$

— 5 equations

$a(\lambda_i)$ — absorption coefficient at λ_i;

$b_6(\lambda_i)$ — backscattering coefficient at λ_i.

$$a(\lambda_i) = a_y(\lambda_i) + a_{ph}(\lambda_i) + a_w(\lambda_i);$$

$$a_g(\lambda_i) = \underline{a_g(440)} \cdot \exp\left[-0.017(\lambda_i - 440)\right];$$

$$a_{ph}(\lambda_i) = \underline{a_{ph}(440)} \cdot \left[a_{ph}(\lambda_i)/a_{ph}(440)\right] = a_{ph}(440) \cdot f(\lambda_i);$$

$f(\lambda_i)$ — from Bricaud et al., 1995 (Chl = 0.5 $\frac{mg}{m^3}$).

$$b_6(\lambda_i) = \underline{b_{6p}(550)} \cdot \left(\lambda/550\right)^{-n} + b_w(\lambda_i);$$

$$\boxed{a_g(440); \; a_{ph}(440); \; b_{6p}(550)} \quad - \text{3 unknowns}$$

$$a_{ph}(440) \longrightarrow C_a;$$

$$k_d(490) = 1.25\left[a(490) + b_6(490)\right].$$

A least square method

$$\sum_i \{X(\lambda_i)\cdot-b_b(\lambda_i)/[a(\lambda_i) + b_b(\lambda_i)]\}^2 = min;$$

$$a(\lambda_i)=exp[-S\ (\lambda_i)-440)]\cdot a_y(440) + a^*_{ph}(\lambda_i)\cdot a_{ph}(440)\cdot + a_w(\lambda);$$

$$b_b(\lambda_i) = 0.5b_{bw}(\lambda_i) + b_{bp}(550)\cdot(550/(\lambda_i)^n;$$

Generally speaking, 5 unknowns:

$$a_y(440),\quad a_{ph}(440),\quad b_{bp}(550);$$

$$S,\quad n.$$

We deal with an inverse problem which solution can be unstable; that is small errors in the input data can result in great errors in the output values. Instability usually grows with increase of the number of unknowns. In such a situation, the quest for more accurate statement of the bio-optical characteristics with greater number of parameters can have led to a physically absurd solution. To avoid it, the setting of a problem should be optimal. Usually, the parameters S and n are taken as known, and with 5 SeaWiFS spectral bands in visible region we have 5 equations for 3 unknowns.

Correct choice of the S and n parameters

$$S = 0.0192 - 0.0049 \cdot [r_{RS}(412)/r_{RS}(490)]$$
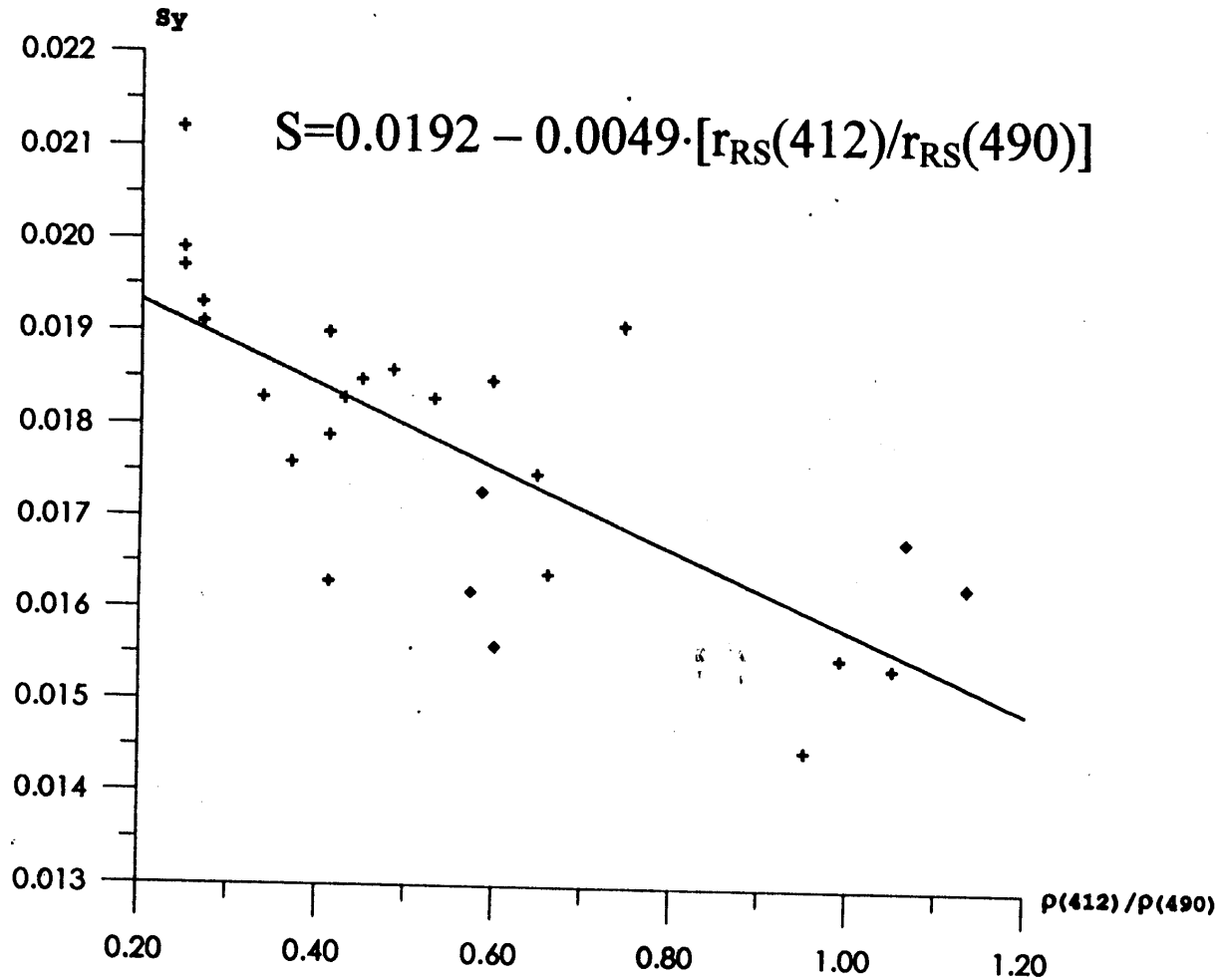
Sy against P(412)/P(490)   (n=27, r^2=0.55)

+ — "Akvanavt'97" $\sigma_{regr} = 0.0008\ \text{nm}^{-1}$.

♦ — Barents Sea

$$n = -1.13 + 2.57 \cdot [r_{RS}(443)/r_{RS}(490)]$$

(Carder et al. 1999)

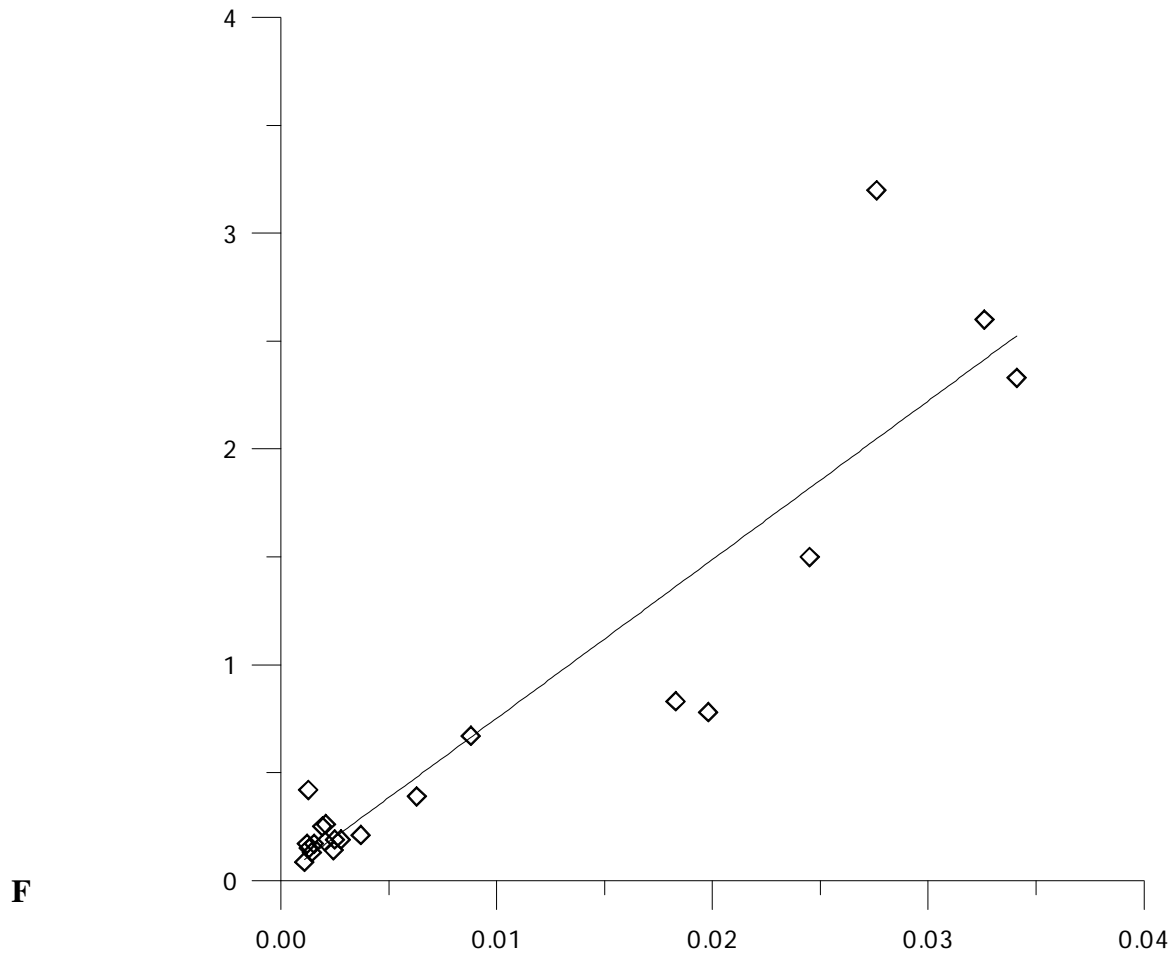# Simplified algorithm to derive the particle backscattering coefficient

$$L_{WN}(555) \rightarrow \tau_{rs}(555) \rightarrow u(555);$$

$$u(555) = \frac{b_B(555)}{a(555) + b_B(555)} = 1.17\, \frac{b_B(555)}{K_d(555)};$$

$$b_{bp}(555) = 0.855\, u(555) \cdot K_d(555) - b_{bw}(555);$$

$$K_d(555) = 0.565 \cdot K_d(490) - 0.0051 \quad - \quad \text{Austin, Petzold, 1984}$$

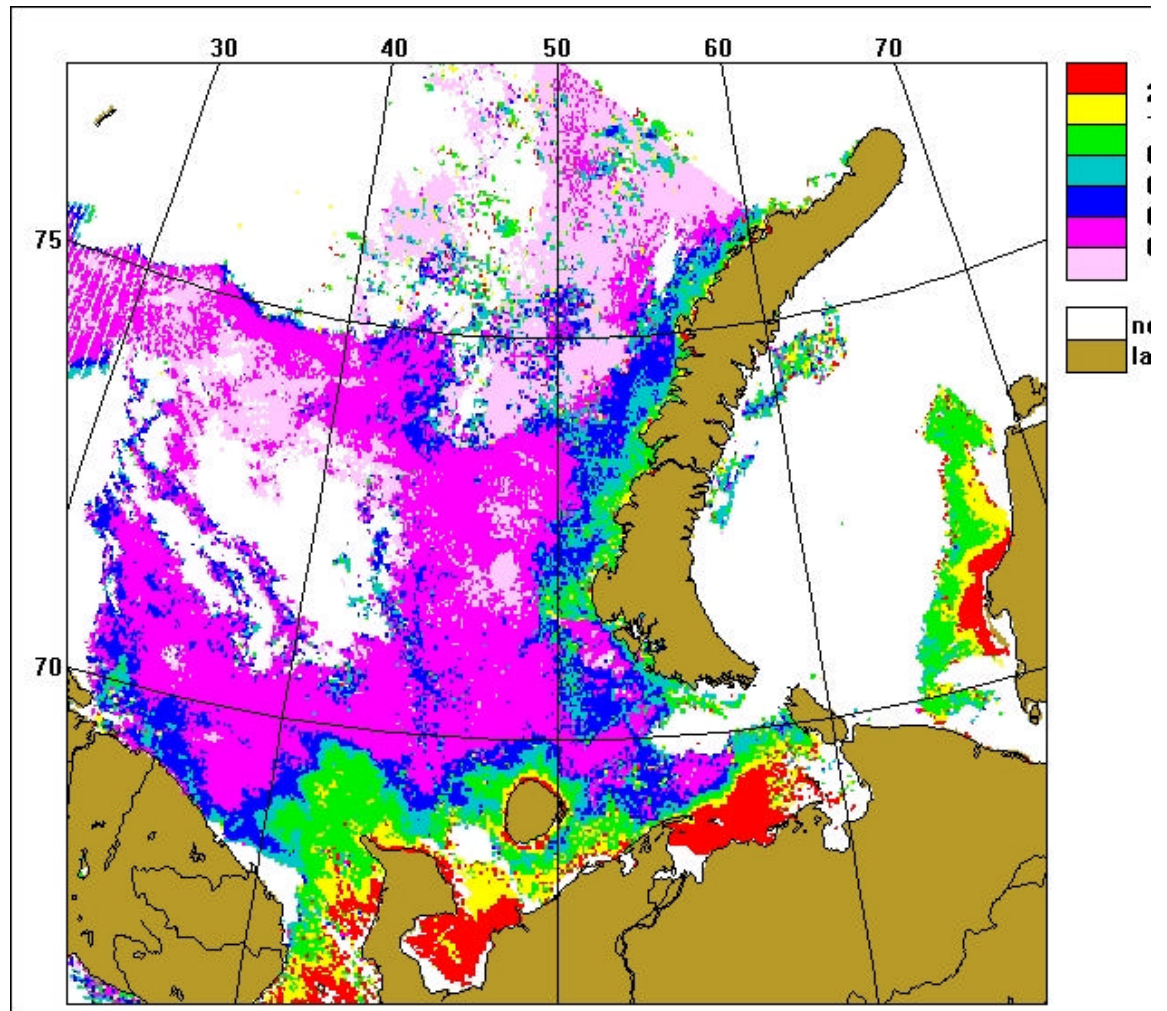$$K_d(490) = 0.19 \cdot \left[L_{WN}(510) \big/ L_{WN}(555) \right]^{-3.0} + 0.022;$$

$$b_{bp}(555) = f\left[L_{WN}(510),\ L_{WN}(555) \right]$$

F

The correlation between the values of $b_{bp}(555)$ calculated with the simplified algorithm (on the abscissa) and concentration $\tilde{N}_s$ of suspended matter (on the ordinate); solid line – the regression equation:

$$\tilde{N}_s = 73.5 \, b_{bp}(555) + 0.016,$$

where $\tilde{N}_s$ in $g \cdot m^{-3}$, $b_{bp}(555)$ in m^{-1}; the regression error is equal to about 30%.

The summer distribution of concentration of suspended matter concentration in the Barents Sea derived from SeaWiFS data in 1999.